Chlorpyrifos remediation in agriculture runoff with homogeneous solar photo-Fenton reaction at near neutral pH: phytotoxicity assessment

Kazem Naddafi, Susana Silva Martinez, Ramin Nabizadeh, Kamyar Yaghmaeian, Seyed Jamaleddin Shahtaheri and Hoda Amiri

ABSTRACT

This study represents the first application of Fe–citrate-based photo-Fenton chemistry for the degradation of chlorpyrifos (CPF) spiked into agricultural runoff, and its phytotoxicity assessment. The effects of the initial CPF concentration, time and ratio of Fe–citrate/H_2O_2 on CPF removal during the photo-Fenton reaction were investigated and modeled with analysis of variance using R software by the response-surface methodology package. According to the stationary point in original units, the optimal condition for 70.00% CPF removal was as follows: CPF = 2.5 mg L^{-1} (0.0), time = 48.0 min (0.585) and Fe–citrate/H_2O_2 = 0.075 (0.539). Beside running the system at near-neutral pH, another strength of this study is related to the treatment of agricultural runoff contaminated with CPF with a raceway pond reactor, which has the advantages of simplicity of the facilities and procedures, as well as the possibility of using sunlight more efficiently in the field of applications. Finally, untreated and treated agriculture runoffs were used as irrigation to determine their phytotoxic effects on seed germination of cress (*Lepidium sativum*). Solar photo-Fenton treatment greatly reduced phytotoxicity of agriculture runoff and showed the highest germination percentage (70%) compared to both raw agricultural runoff (60%) and untreated CPF-spiked runoff (35%).

Key words | chlorpyrifos, germination index, iron-citrate, organophosphorus pesticide, photo-Fenton

HIGHLIGHTS

- The study is the first application of Fe–citrate-based photo-Fenton chemistry for the degradation of chlorpyrifos spiked into agricultural runoff.
- Treatment of agricultural runoff contaminated with CPF with a solar raceway pond reactor is a promising application of this system in the field.
- The phytotoxicity result of the final effluent also showed a good potential for agriculture runoff reuse in irrigation.

Kazem Naddafi
Ramin Nabizadeh
Kamyar Yaghmaeian
Department of Environmental Health Engineering, School of Public Health,
Tehran University of Medical Sciences,
Tehran, Iran

Kazem Naddafi
Ramin Nabizadeh
Center for Air Pollution Research (CAPR), Institute for Environmental Research (IER),
Tehran University of Medical Sciences,
Tehran, Iran

Susana Silva Martinez
Centro de Investigación en Ingeniería y Ciencias Aplicadas,
Av. Universidad 1001, Col. Chamilpa,
Cuernavaca, Mor., Mexico

Kamyar Yaghmaeian
Center for Solid Waste Research, Institute for Environmental Research,
Tehran University of Medical Sciences,
Tehran, Iran

Seyed Jamaleddin Shahtaheri
Department of Occupational Health Engineering, School of Public Health, Institute for Environmental Research,
Tehran University of Medical Sciences,
Tehran, Iran

Hoda Amiri (corresponding author)
Environmental Health Engineering Research Center,
Kerman University of Medical Sciences,
Kerman, Iran
and
Department of Environmental Health, School of Public Health,
Kerman University of Medical Sciences,
Kerman, Iran
E-mail: *hoda.amiri@gmail.com*; *Hoda.Amiri@kmu.ac.ir*

INTRODUCTION

Chlorpyrifos (CPF) can be detected in water in a fairly wide range depending on the use of this pesticide in a given area: from 2.86 ng L^{-1} in natural water to near its water solubility (2 mg L^{-1}) (Herrero-Hernández *et al.* 2013; Ccanccapa *et al.* 2016; Claver *et al.* 2006; Estevez *et al.* 2016). It appears to be a persistent pesticide that shows genotoxicity and mutagenicity according to several studies. These compounds are mainly those that are persistent with a half-life of more than 2 months in water, bioaccumulate, and have the potential for long-range environmental transport and adverse

doi: 10.2166/wst.2020.556

effects on human health or the environment. The data on carcinogenicity are equivocal. There are a number of epidemiological studies that indicate that the Dursban CPF formulation can be carcinogenic in humans, the strongest association being for lung and rectum cancers (Watts 2012; EPA 2017). Pesticides are frequently found in influents and also in effluents of wastewater treatment plants that usually do not apply advanced chemical oxidation processes. To reduce the potential health risks, several treatment processes have been investigated to remove pesticides from aqueous matrices, including biological treatment (with low removal efficiency), photocatalysis, electrochemical degradation, Fenton oxidation, hydrogen peroxide oxidation, and plasma discharge, as well as physicochemical techniques that include adsorption, membrane technology, ozone, ozone/ultraviolet (UV) photolysis UV photolysis, and ultrasound (Bahena & Martínez 2006; Hoseini *et al.* 2016; Chavoshani *et al.* 2018; Fatima *et al.* 2019; Liu *et al.* 2019; Malakootian *et al.* 2019b; Patel *et al.* 2019; Malakootian *et al.* 2020).

Among them, the conventional Fenton process, which involves the production *in situ* of hydroxyl radicals (˙OH) by ferrous iron and hydrogen peroxide (H_2O_2), stands out for its high efficiency in the degradation of organic matter, operational simplicity, low cost and environmentally friendly process (Hashemi *et al.* 2018; Dutta *et al.* 2019; Heidari *et al.* 2019; Malakootian *et al.* 2019a; Malakootian & Heidari 2020). Despite its advantages, this process has not been widely used, due to the requirement for acidic conditions and the high and rapid consumption of H_2O_2 (which represents the main cost of the process) and iron (Zhang *et al.* 2019).

The first limitation can be solved by iron chelating agents such as ethylene-diaminete-tetraacetic acid, nitrilotriacetic acid, oxalate, citrate and malonate. The resulting iron complexes maintain the solubility of Fe^{3+}/Fe^{2+} over a wide pH range and exhibit high absorbance in the UV-vis region. The iron–citrate complex is a good alternative for the solubilization of iron in Fenton processes due to its low toxicity and global formation constant (log ß = 14.29), and it being easily available and applicable to high pH values of up to 9.0. The electro-Fenton (EF) process, where H_2O_2 is generated directly at the cathode from the reduction of dissolved O_2 plus ferrous iron as a catalyst in low concentrations, has been reported as a suitable alternative to overcome the second disadvantage of conventional Fenton (Ou *et al.* 2008; Manenti *et al.* 2015; Ruales-Lonfat *et al.* 2016). The aim of this research is to study the CPF degradation capacity of the iron–citrate complex in Fenton and photo-Fenton treatments under simulated solar lighting, at near-neutral pH in agricultural runoff under real conditions in a raceway pond reactor (RPR) as a powerful and inexpensive extensive photoreactor. When the treatment is directed to the oxidation of microcontaminants, the concentration of the contaminant is at least a thousand times less than that of the oxidation of macrocontaminants. Therefore, the process needs less oxidant species (mainly OH˙ radicals) and, consequently, less irradiation (less photons) to achieve elimination. Until our study, no cases have been published for RPR photocatalyst applications that use sunlight which have been widely applied for microalgal mass culture and pesticide degradation and no study for CPF using the Fenton process. For this, a laboratory-scale RPR was designed as an alternative treatment technology to investigate the influence of the concentration of CPF and the ratio of Fe–citrate/H_2O_2 on the degradation of CPF at near-neutral pH (6.8 ± 0.3) under simulated sunlight.

MATERIALS AND METHODS

Chemicals

Chlorpyrifos (analytical grade) was purchased from Dr Ehrenstorfer (Germany, > 99%purity). Ferric-citrate (Fe–citrate) was provided by Sigma-Aldrich. Acetonitrile (chromatography grade) was provided by Merck (Darmstadt, Germany). Acetonitrile was used for preparation of CPF stock solutions (1,000 mg L^{-1}). Several concentrations of CPF solutions (1–4 mg L^{-1}) were spiked into the agricultural effluent.

Runoff wastewater and experimental conditions

Several experiments were carried out in an RPR using real agricultural runoff from a farm land in Tehran, Iran. The characteristics of the agricultural runoff are shown in Table 1. The runoff was collected, acidified to pH 2.8 with sulfuric acid and used within 5 days. The small-scale RPR used to carry out the experiments has been reported in our previous work (Amiri *et al.* 2018), and is shown in the schematic representation (Figure 1). Briefly, the RPR consists of a fiberglass container (50 cm × 15 cm × 10 cm) separated by a central wall, forming two channels with a capacity of 7.5 L. It also has a motorized paddlewheel that uniformly maintains a mixed flow of a homogeneous system during the process and a halogen lamp (300 W, Osram, Munich, Germany, wavelength

Table 1 | Characterization of the real agricultural runoff

Parameters	Concentration	Parameters	Concentration
pH	6.8 ± 0.3	Conductivity	420 ± 0.8 μS cm^{-1}
Total dissolved solids (TDS)	210 ± 0.94 mg L^{-1}	Total phosphorus	0.34 ± 01 mg L^{-1}
Total nitrogen	1.8 ± 0.16 mg L^{-1}	Salinity	0.22 ±0.02 mg L^{-1}

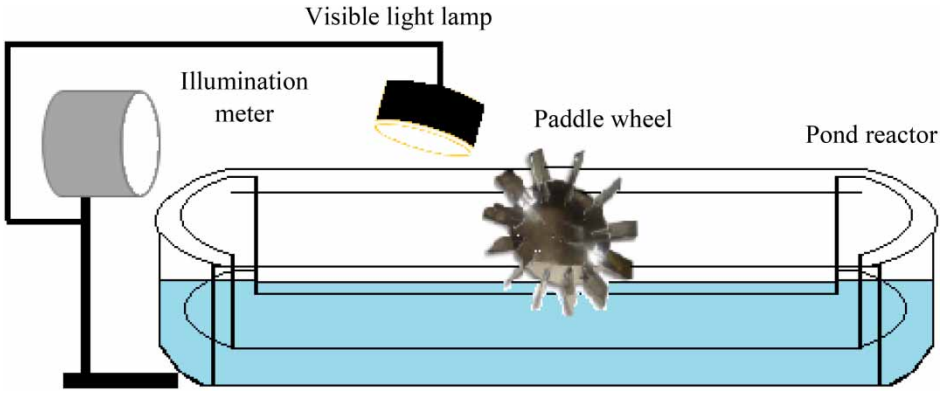

Figure 1 | Schematic representation of the fiberglass raceway pond reactor.

range: 400–800 nm) as visible light source for the photocatalytic reactions that take place in the solution exposed for up to 1 h. An illumination meter (LX-100S, KIMO, France) was used to measure the luminous intensity (lux), which was then converted to the irradiance unit (in W m^{-2}) using conversion factors (Thimijan & Heins 1983). An aqueous aliquot of 2.5 L of the agricultural effluent, spiked with CPF at near-neutral pH (6.8 ± 0.3), was placed in the RPR. The estimated light intensity was 697 ± 5.33 lux (7.5×10^{-3} W m^{-2}), which is much lower than the global average solar irradiance (~10 W m^{-2}) (Mendoza *et al.* 2017).

Analytical determinations

The CPF concentration of each sample was analyzed using a Varian chrome pack CP–3800 gas chromatograph as reported previously (Amiri *et al.* 2018). Total nitrogen and total phosphorus were measured using a Hach test kit (Germany). Total iron concentration (unfiltered and filtered with a 0.45 μm diameter polytetrafluoroethylene syringe-driven filter) was measured using the method of 1,10-phenanthroline following ISO 6332 (ISO 1988); H_2O_2 was measured using ammonium metavanadate following Pupo Nogueira and co-workers' method (Nogueira *et al.* 2005).

Experimental design

The experimental variables that influence the degradation of CPF were determined by half fractional factorial design. A central composite design (CCD) was then executed for three independent variables to design the experiments. A five level, three variables central composite rotatable design was employed for the optimization with respect to three important reaction variables: CPF concentration (X_1), time (X_2) and Fe–citrate/H_2O_2 (X_3). Design generation and statistical analysis were performed using the R software by the response-surface methodology (RSM) package. RSM comprises a set of methods to explore the optimal operating conditions through experimental methods (Lenth 2009; Amiri *et al.* 2018).

According to Equation (1), the actual value of an independent variable converts to its coded form (X1–X3) by calculating the statistical value:

$$X \sim (Xi - M)/R \quad (1)$$

where X, Xi, M and R are the coded value of the *i*th independent variable, actual value, mean of actual value ((min + max)/2)) and range of actual value ((max – min)/2)), respectively. According to the Montgomery method (Amiri *et al.*

2018), the total number of experiments carried out was 23, as shown in Table 2. The empirical second-order polynomial model was used to create a prediction model by the experimental data (Naddafi *et al.* 2018).

Phytotoxicity assessment

This experiment was performed following the methodology described by Jaafarzadeh *et al.* (2017). Briefly, 10 mL of treated and untreated CPF spiked into agricultural runoff, or control solutions (ultrapure water and raw agricultural runoff), was added to Petri dishes with one layer of filter paper. Then, 30 cress (*Lepidium sativum*) seeds, disinfected with sodium hypochlorite followed by washing 10 times with de-ionized water, were added to each Petri dish and incubated in the dark at 24°C (± 2°C) for 72 h. The germination index (GI) (%) was calculated according to the following equation

$$\mathrm{GI}(\%) = 100 \times \left(\frac{\text{seed germination} \times \text{root length of the sample}}{\text{seed germination} \times \text{root length of the control}}\right)$$

Statistical analysis

Using R software (3.0.3), multiple regression was chosen to the generalized minimum square to find the relationship between independent and dependent variables. Moreover, the stationary point in original units was used, as a result of the analysis of the variance table in the R software, to estimate an optimal condition for the removal of CPF.

Table 2 | Actual and coded values of independent variables used for the experimental design (CCD)

	Coded variables			Actual variables			Response	
Run order	X1	X2	X3	CPF (mg L^{-1})	Time (min)	Fe–citrate/H_2O_2	Experimental (%)	Predicted (%)
1	0.00	0.00	0.00	2.50	32.00	0.05	41.56	40.12
2	0.00	0.00	0.00	2.50	32.00	0.05	35.11	40.12
3	0.00	0.00	0.00	2.50	32.00	0.05	42.00	40.12
4	−0.59	0.59	−0.59	1.60	49.00	0.02	39.08	40.50
5	0.59	−0.59	0.59	3.40	16.00	0.08	28.45	29.13
6	0.59	−0.59	−0.59	3.40	16.00	0.02	5.01	2.63
7	0.59	0.59	0.59	3.40	49.00	0.08	69.71	71.23
8	−0.59	−0.59	0.59	1.60	16.00	0.08	22.10	25.61
9	−0.59	0.59	0.59	1.60	49.00	0.08	68.09	72.62
10	0.00	0.00	0.00	2.50	32.00	0.05	45.03	40.12
11	0.00	0.00	0.00	2.50	32.00	0.05	43.12	40.12
12	0.00	0.00	0.00	2.50	32.00	0.05	39.00	40.12
13	0.00	0.00	0.00	2.50	32.00	0.05	42.50	40.12
14	0.00	0.00	0.00	2.50	32.00	0.05	41.80	40.12
15	0.59	0.59	−0.59	3.40	49.00	0.02	20.00	19.21
16	−0.59	−0.59	−0.59	1.60	16.00	0.02	19.00	19.01
17	0.00	0.00	0.00	2.50	32.00	0.05	36.01	40.12
18	0.00	0.00	−1.00	2.50	32.00	00.00	0.00	2.70
19	0.00	0.00	+1.00	2.50	32.00	0.10	58.95	52.39
20	1.00	0.00	0.00	4.00	32.00	0.05	33.02	34.54
21	−1.00	0.00	0.00	1.00	32.00	0.05	55.03	49.60
22	0.00	−1.00	0.00	2.50	5.00	0.05	8.33	9.07
23	0.00	1.00	0.00	2.50	60.00	0.05	66.35	62.96

RESULTS AND DISCUSSION

Model fitting and statistical analysis

Box and Wilson developed the CCD, which corresponds to one of the most popular response-surface designs (Lenth 2009). It is a first-order (2N) design augmented by additional center and axial points to allow the estimation of the tuning parameters of a second-order model. According to the design created, 23 experiments were performed for the Fenton solar treatment process.

Table 2 presents the independent variables and experimental and predicted results for CPF degradation. A quadratic model was chosen among several verified models as the best for CPF oxidation percentage. According to Table 3, the model coefficient for the response was estimated using the multiple regression analysis technique included in the RSM. Also from the analysis of variance (ANOVA), it is clear that the linear coefficients (X1, X2, X3), second-order (two-way interaction (X1:X3, X2:X3)) and pure quadratic terms ($X2^2$, $X3^2$) contribute significantly to the model, so the canonical analysis is relevant.

The quadratic model thus obtained is given by Equation (2)

$$\begin{aligned} &Y\ (\text{CPF removal}\ (\%)) \\ &= 40.1190 - 7.5298{*}X1 + 25.4978{*}X2 + 24.8431{*}X3 \\ &\quad - 3.5266{*}X1{*}X2 + 14.2927{*}X1{*}X3 + 18.3277{*}X2{*}X3 \\ &\quad + 2.6838{*}X1^2 - 6.9079{*}X2^2 - 11.8408{*}X3^2 \end{aligned} \quad (2)$$

R^2 and *p*-value for lack of fit are two important parameters to investigate the fitness of the model. Table 4 presents the ANOVA result of the model for CPF degradation. It is clear that the predicted model (R^2) satisfactorily explains 97.5% of the total variations. In addition, R^2-adjusted value of 0.984 indicates the high degree of correlation between the observed and predicted values for the efficiency of CPF removal in the model. With regard to the lack of fit, as a critical parameter of the validation of the model, the fitness of the model is confirmed without significant differences between the observed and predicted model data (*p*-value of lack of fit > 0.05). A very high F-value (F-statistic = 56.53, much higher than unity) and a very low probability value (*p*-value = 5.835 ×10−9) indicate that the model obtained was highly significant.

Table 3 | Coefficient of quadratic model using CCD

Coefficients	Estimate	SE	t	p	
(Intercept)	40.1190	1.2796	31.3533	1.233×10^{-13}	***
X1	−7.5298	1.7383	−4.3316	0.0008142	***
X2	25.4978	1.7379	14.6718	1.813×10^{-9}	***
X3	24.8431	1.7383	14.2914	2.504×10^{-9}	***
X1:X2	−3.5266	3.7695	−0.9356	0.3665542	
X1:X3	14.2927	3.7706	3.7906	0.0022472	**
X2:X3	18.3277	3.7695	4.8621	0.0003104	***
$X1^2$	2.6838	2.7139	0.9889	0.3407594	
$X2^2$	−6.9079	2.7163	−2.5432	0.0245066	*
$X3^2$	−11.8408	2.7139	−4.3630	0.0007684	***

p value: 0 '***' 0.001 '**' 0.01 '*' 0.05 '.' 0.1 '1'. where: SE = standard error, t = student test, *p* = probability.

Table 4 | Analysis of variance regression for CPF removal using solar photo-Fenton

Model formula	Df	Sum Sq	Mean Sq	F-value	Pr (>F)
First-order response	3	6535.5	2178.49	147.7893	2.706×10^{-10}
Two way interaction	3	573.2	191.05	12.9611	0.000333
Pure quadratic response	3	390.4	130.12	8.8275	0.001878
Residuals	13	191.6	14.74		
Lack of fit	5	103.5	20.70	1.8799	0.203745
Pure error	8	88.1	11.01		

Note: multiple R^2: 0.9751, adjusted R^2: 0.9578, F-statistic: 56.53 on 9 and 13 degrees of freedom (Df), *p*-value: 5.835×10^{-9}. Sum Sq: sum of squares; Mean Sq: mean squares.

Removal of CPF by photo-Fenton process

The CPF degradation efficiency can be greatly reduced by excess or deficiency of hydrogen peroxide and iron in the Fenton process. In addition, the use of appropriate reagent concentrations will affect both economic and aesthetic aspects by preventing additional operating costs due to the excessive use of reagents and will moderate the difficulties encountered in removing excess iron to achieve effluent standards. Although H_2O_2 is an essential parameter for the creation of $OH^{\cdot}$ radicals, its high concentration acts as a radical scavenger and performs a self-decomposition to O_2 and H_2O that causes a reduction in efficiency. Thus, the use of adequate concentrations of hydrogen peroxide and iron in the Fenton process is important. The water matrix used in the experiments contained 1.8 ± 0.16 mg L^{-1} and 0.34 ± 0.1 mg L^{-1} of total nitrogen and total phosphorus respectively with a conductivity of 420 ± 0.8 µS cm^{-1}. Therefore, some of the hydroxyl radicals generated during the treatment were expected to

react with organic molecules other than the target compounds. Consequently, the presence of all these species and compounds in the runoff should be taken into account, as they generally slow down the reaction rate compared to water containing less organic matter and inorganic constituents (Naddafi *et al.* 2018).

Fe–citrate concentration

The effect of Fe–citrate concentration on the degradation efficiency of CPF (2.5 mg L^{-1}) was conducted in the presence of 0.2, 0.5, 0.8 and 1.0 mg L^{-1} of iron with 10 mg L^{-1} of H_2O_2. It was observed that the degradation percentage improved with increasing reagent and time, until the Fe–-citrate/H_2O_2 ratio increased to more than 0.08, as shown in Figure 2. The 3D response-surface and 2D contour plots in Figure 3 visualize the relationship between CPF removal as response and experimental levels of variables (CPF, time, Fe–citrate/H_2O_2) and their interactions. The response-surface plots show that at low and high levels of Fe–citrate/H_2O_2 ratios, CPF oxidation was minimal. The literature confirms that the Fe/H_2O_2 ratio higher than 0.10 may decrease the efficiency of contaminant removal due to the scavenging of hydroxyl radicals (Mirzaei *et al.* 2017).

Assessment of CPF concentration with time

In this study, we tried to simulate the real condition of agricultural runoff contaminated with CPF on a pilot plant scale. The CPF degradation is visualized through the contour plot and the 3D view of response-surface plots (Figure 3). The plots were represented based on two factors: CPF and Fe–citrate/H_2O_2 ratio, with the time kept at a fixed level (37.78 min); and CPF and time, holding Fe–citrate/H_2O_2 ratios at a fixed level (0.05). As can be seen in this figure, the efficiency of CPF degradation was reduced by increasing its concentration, while time has a positive effect on the solar photo-Fenton process. This occurs because high concentrations of CPF require higher concentrations of oxidant species (hydroxyl radicals, ferryl complexes, etc.) for effective removal. Therefore, at a constant level of other operating parameters, the generated oxidant species do not meet the demand for additional contaminant input concentration. In addition, in the Fenton reaction, when the concentration of CPF increases, the number of active sites, where radical reactions take place, is limited, which reduces the absorption of light by hydrogen peroxide in the Fenton photocatalytic reaction. However, the generation of $OH^{\cdot}$ radicals and other oxidant species is retained and as a consequence the removal efficiency decreases.

Mechanism of CPF removal in the system

The equilibrium Fe(III) speciation within the pH range of 4.6–8.0 is $FeCit^{-}$ (Hamm *et al.* 1954; Zepp *et al.* 1992; Faust & Zepp 1993; Hug *et al.* 2001; Ou *et al.* 2008). The mechanism of the homogeneous solar photo-Fenton degradation of CPF in the presence of Fe(III)-citrate species

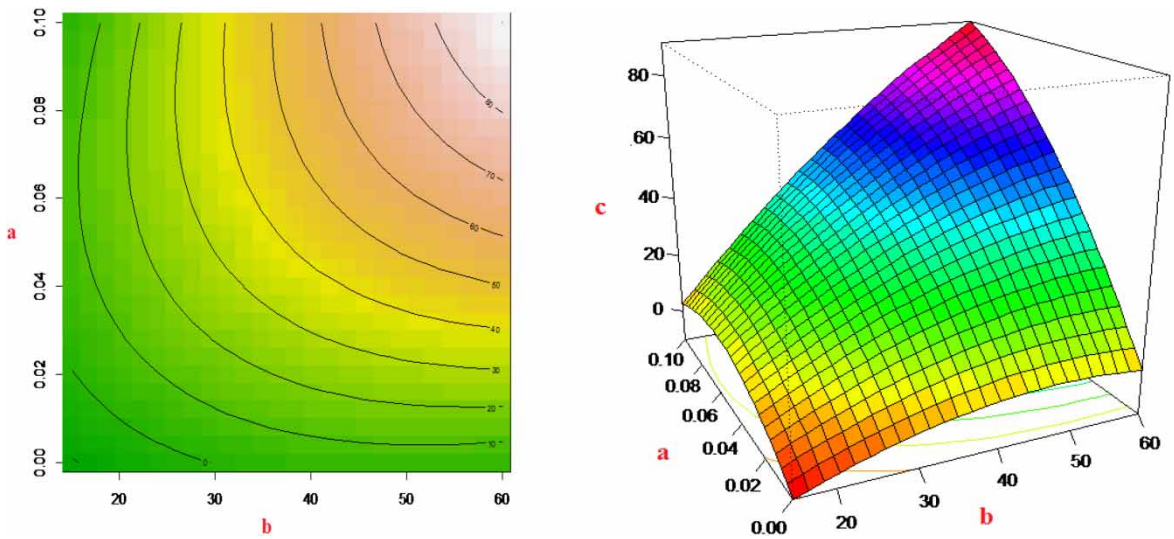

Figure 2 | Design-expert plot: response-surface contour (left) and 3D (right) plots near the stationary point for CPF removal (%) at pH = 6.8 ± 0.3. a: Fe–citrate /H_2O_2 ratio, b: time (min) and c: removal efficiency (%).

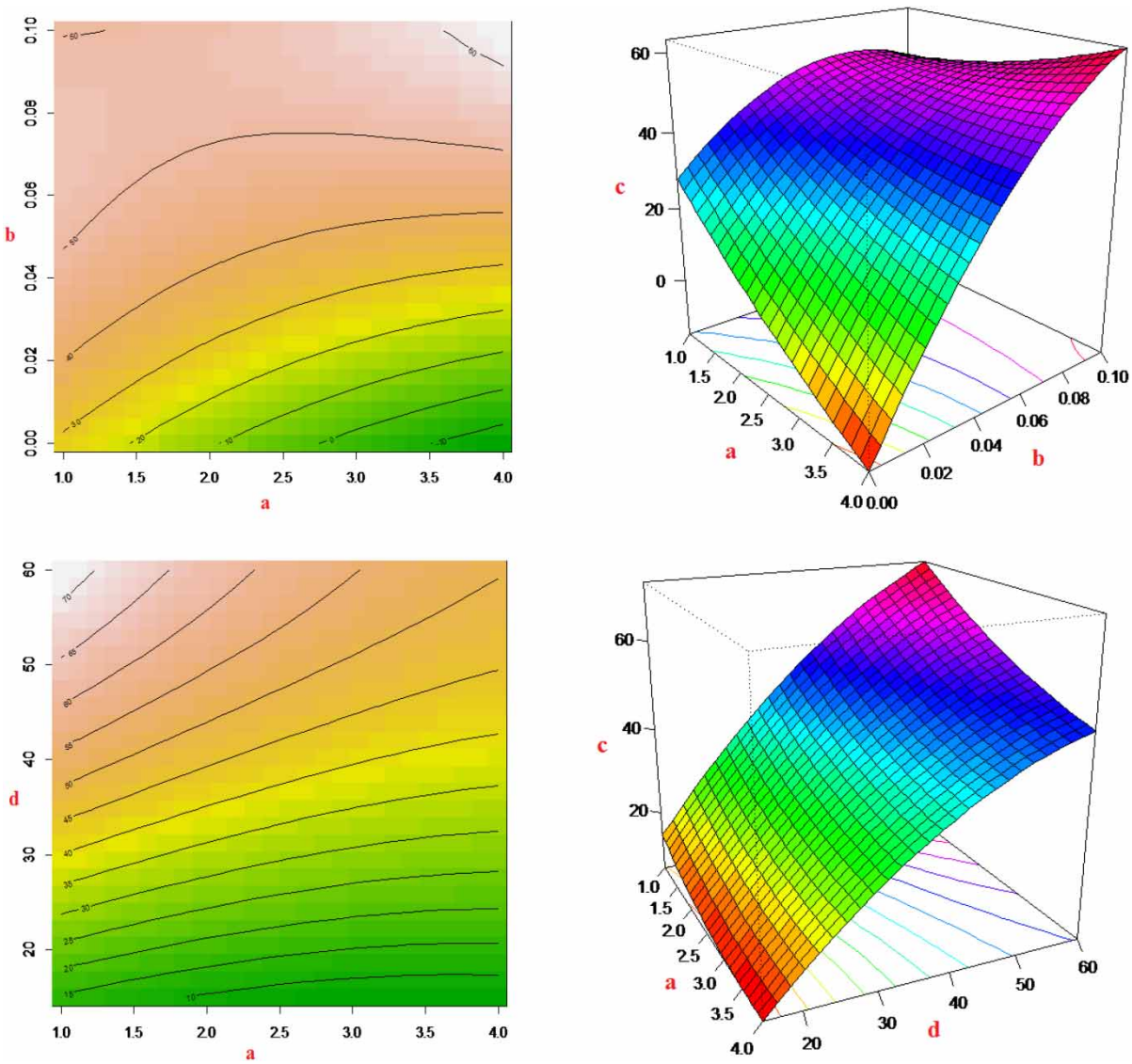

Figure 3 | Design-expert plot: response-surface contour (left) and 3D (right) plots near the stationary point for CPF removal (%) at pH = 6.8 ± 0.3. a: Initial CPF concentration (mg L^{-1}), b: Fe–citrate/H_2O_2 ratio, c: removal efficiency (%) and d: time (min).

($Fe(OH)Cit^{-}$) involves several reaction processes, such as the following.

(a) Photochemical redox reactions of $Fe(OH)Cit^{-}$ produce Fe(II) and the citrate radical $Cit^{\bullet 2-}$ ($HO\text{-}CR_2\text{-}COO^{\bullet}$ with $R = \text{-}CH_2COO^{-}$) (Hug *et al.* 2001) followed by decarboxylation to the carbon centered 3-hydroxo-glutarate radical, $3\text{-}HGA^{\bullet 2-}$ ($HO\text{-}^{\bullet}CR_2$), which reacts with O_2 to form various oxidants such as $OH^{\bullet}$, $O_2^{\bullet -}/HO_2^{\bullet}$ and H_2O_2 (Faust & Zepp 1993; Anfossi *et al.* 2006) eliminating the CPF from the aqueous system. Other competing reactions can also take place with the citrate radical such as back-reaction with Fe(II) to re-form Fe(III) or the reduction of $Fe(OH)Cit^{-}$ species (Faust & Zepp 1993).

(b) The reaction of Fe(II) species, photochemically produced, with H_2O_2 at neutral pH might not result in $OH^{\bullet}$ radical formation (Rush *et al.* 1990) but in the formation of Fe(IV) species (Koppenol & Liebman 1984). There is evidence that many Fe(II) and Fe(III) chelates (such as citrate, L) react thermally with H_2O_2 to form ferryl complexes, (L)Fe(IV) = O, or one electron ligand-oxidized ferryl complexes, ($L^{+\bullet}$)Fe(IV) = O. These species, like $OH^{\bullet}$ radicals, can be strong and nonselective oxidizing agents (Leising *et al.* 1991; Sun & Pignatello 1993).

(c) Direct photolysis of H_2O_2 produces $OH^{\bullet}$; however, this production process is comparatively slow because H_2O_2 weakly absorbs solar irradiation.

Thus, it is expected that $OH^{\bullet}$ and ferryl complexes are responsible for the homogeneous solar photo-Fenton degradation of CPF.

Validation of the model

The optimal oxidation conditions (X1 = 2.5 mg L^{-1} (0.0), X2 = 48.0 min (0.585) and X3 = 0.075 (0.539)) for CPF removal were suggested by the variance analysis table of the R software. The theoretical CPF removal that was predicted under the above conditions was 70.00%. This set of conditions was determined as optimal by the RSM optimization approach and was used to experimentally validate and predict the values of the responses using the model equation. The mean removal efficiency for CPF was 65 ± 1.03% ($n = 3$), which corresponds well to the predicted value of the model equation, confirming that the response model was adequate for optimization.

Phytotoxicity evaluation

The toxicity tests following by treatment process are critical in the evaluation of effluent quality. Hence, both untreated and treated agriculture runoff were assessed for their phytotoxicity. The result for cress seed germination inhibition upon exposure to different concentration of CPF in runoff is given in Figure 4. Treated agricultural runoff showed highest germination percentage (70%) compared to both raw agricultural runoff (60%) and untreated CPF-spiked runoff CPF spiking (35%). This result can be attributed to the formation of non-toxic oxidation intermediates, which were not toxic to *Lepidium sativum*. In addition, iron ions (nutrients) present in the iron–citrate complex might have contributed to the germination. Regarding the results of cress seed germination, as the most sensitive plant (Jaafarzadeh *et al.* 2017), the final effluent has a good potential for water reuse in irrigation.

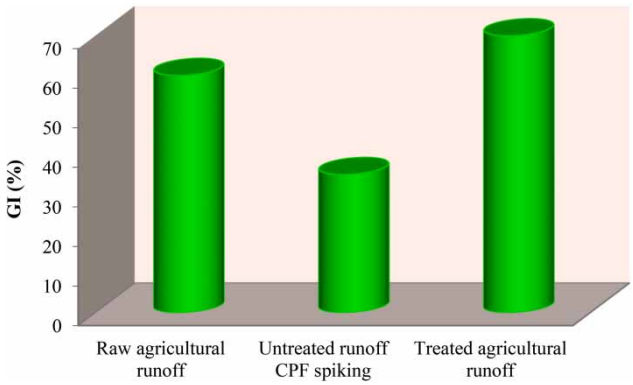

Figure 4 | The germination index (%) of different runoff conditions.

Critical comparison of Fenton reaction for CPF degradation

Previous works reported the influence of Fenton reagent on CPF degradation. For instance, Affam and collaborators (Affam *et al.* 2012) investigated the effect of the Fenton process on the degradation of an effluent containing a mixture of three pesticides: of chlorpyrifos (initial concentration (Co) = 100 mg L^{-1}), cypermethrin (Co = 50 mg L^{-1}) and chlorothalonil (Co = 250 mg L^{-1}), and reported a chemical oxygen demand (COD) and total organic carbon (TOC) removal of 69.03 and 55.61%, respectively, in 60 min reaction. In addition, these authors (Affam *et al.* 2014) examined the effect of UV Fenton pretreatment operating conditions combined with the aerobic sequencing batch reactor (SBR) on degradation and biodegradability (biochemical oxygen demand/COD ratio) improvement of chlorpyrifos (Co = 805.56 ± 10.0 mg L^{-1}), cypermethrin (Co = 105.75 ± 10.0 mg L^{-1}) and chlorothalonil (Co = 692.08 ± 10.0 mg L^{-1}) pesticide wastewater under optimal condition (as shown in Table 5); a higher COD and TOC removal was reported for the UV Fenton-SBR treatment. Saini & Kumar (2016) used the Fenton oxidation process for the degradation of 30 mg L^{-1} of CPF, reporting an efficiency removal of CPF of 94% with a COD decrease of 83.51% in 60 min of reaction time. In addition, Augustine *et al.* (2016) examined solar irradiation to enhance Fenton treatment of CPF pesticide wastewater with an initial concentration of 200 mg L^{-1} finding a TOC decrease of 89.20% in 60 min of reaction time. It is important to mention that the solubility of CPF in water is 2 mg L^{-1}. Therefore, CPF concentrations higher than 4 mg L^{-1} create a milky solution that interferes with both the treatment process and the measurement method using high-performance liquid chromatography or gas chromatography by reducing the repeatability and accuracy of the experiments. The documents mentioned (Table 5) that have examined the degradation of initial CPF concentrations above 4 mg L^{-1} appear to be far from the natural condition and should be considered more in relation to their results. This present study reports the

Table 5 | Comparison between Fenton treatment technologies related to chlorpyrifos degradation

Pesticide	Initial concentration	Fenton features	Removal efficiency	Reference
Chlorpyrifos	CPF = 4 mg L^{-1} Salinity = 0.22 ±0.02 mg L^{-1} TDS = 210 ± 0.94 mg L^{-1} Total nitrogen = 1.8 ± 0.16 mg L^{-1} Total phosphorus = 0.34 ± 01 mg L^{-1}	pH = 6.8 ± 0.3 H_2O_2:Fe–citrate 10:0.75	Reaction time = 48 min; CPF = 65 ± 1.03%	Present study
Chlorpyrifos	COD = 1,330 mg L^{-1}	pH = 3, H_2O_2 dosing rate 120 mg min^{-1}, $[Fe^{2+}]_0$ = 5.0 mM.	Reaction time = 70 min; COD = 77.00%	Samet *et al.* (2012)
Chlorpyrifos, cypermethrin, chlorothalonil	CPF = 100 mg L^{-1}, cypermethrin = 50 mg L^{-1}, chlorothalonil = 250 mg L^{-1}.	pH = 3 H_2O_2:COD 3:1 H_2O_2:Fe^{2+} 10:1	UV Fenton (60 min) COD = 69.03% TOC = 55.61%	Affam *et al.* (2012)
Chlorpyrifos, cypermethrin, chlorothalonil	CPF = 805.56 ± 10.0 mg L^{-1}, cypermethrin = 105.75 ± 10.0 mg L^{-1}, chlorothalonil = 692.08 ± 10.0 mg L^{-1}, COD = 3,350.0 ± 100 mg L^{-1} TOC = 2,960.0 ± 100 mg L^{-1}	pH = 3 H_2O_2:COD 2:1 H_2O_2:Fe^{2+} 25:1	UV Fenton (60 min)COD = 64.8% TOC = 45.9% UV Fenton-SBR (40 d operation at 12 h hydraulic retention time COD = 96.2% TOC = 97.4%	Affam *et al.* (2014)
Chlorpyrifos	CPF = 30 mg L^{-1}, COD = 385 mg L^{-1}.	pH = 3, H_2O_2 = 0.571 mol L^{-1}, Fe^{2+} = 3 g L^{-1}	Reaction time = 60 min; CPF = 94% COD = 83.51%	Saini & Kumar (2016)
Chlorpyrifos	CPF = 200 mg L^{-1}.	pH = 3 H_2O_2:COD 2.5:1 H_2O_2:Fe^{2+} 10:1	Reaction time = 60 min; TOC = 89.20%	Augustine *et al.* (2016)

first application of Fe–citrate-based photo-Fenton chemistry for the degradation of 4 mg L^{-1} of CPF at pH = 6.8 with a CPF removal efficiency of 65 ± 1.03% in 48 min of reaction time using agricultural runoff polluted with CPF. Our results compete with those reported in the literature, showing an important advantage in the almost neutral pH (6.8) used compared to the common pH = 3 used in Fenton processes.

CONCLUSIONS

The solar photo-Fenton process with iron–citrate showed promising results for CPF remediation at near-neutral pH conditions, with the use of a low iron concentration (Fe–citrate concentration: 0.75 mg L^{-1} relative to the Fe content) and avoiding precipitation of ferric hydroxides. This study reports the first application of photo-Fenton chemistry based on Fe–citrate for CPF degradation. Photo-degradability of CPF (2.5 mg L^{-1}) increased from zero to 80% in 60 min by increasing reagent ratio from 0 to 0.1. Under the optimum operating conditions (CPF = 2.5 mg L^{-1}, and Fe–citrate/H_2O_2 = 0.075), 70.00% degradation of the CPF occurred in 48 min.

Another promising application of this system is related to the treatment of agricultural runoff contaminated with CPF in an RPR, because of the simplicity of the facilities and procedures, as well as the possibility of using sunlight more efficiently in field applications. The phytotoxicity result of the final effluent also showed a good potential for agriculture runoff reuse in irrigation section.

ACKNOWLEDGEMENTS

The authors wish to thank the Tehran University of Medical Sciences for the financial support to carry out this project (No. 95-01-46-31412).

DATA AVAILABILITY STATEMENT

All relevant data are included in the paper or its Supplementary Information.

REFERENCES

Affam, A. C., Chaudhuri, M. & Kutty, S. R. M. 2012 Fenton treatment of chlorpyrifos, cypermethrin and chlorothalonil pesticides in aqueous solution. *Journal of Environmental Science and Technology* **5**, 407–418.

Affam, A. C., Chaudhuri, M., Kutty, S. R. M. & Muda, K. 2014 UV Fenton and sequencing batch reactor treatment of chlorpyrifos, cypermethrin and chlorothalonil pesticide wastewater. *International Biodeterioration & Biodegradation* **93**, 195–201.

Amiri, H., Nabizadeh, R., Silva Martinez, S., Jamaleddin Shahtaheri, S., Yaghmaeian, K., Badiei, A., Nazmara, S. & Naddafi, K. 2018 Response surface methodology modeling to improve degradation of Chlorpyrifos in agriculture runoff using TiO_2 solar photocatalytic in a raceway pond reactor. *Ecotoxicology and Environmental Safety* **147**, 919–925.

Anfossi, L., Sales, P. & Vanni, A. 2006 Degradation of anilinopyrimidine fungicides photoinduced by iron (III)–polycarboxylate complexes. *Pest Management Science* **62**, 872–879.

Augustine, A. C., Chaudhuri, M. & Hetrick, K. 2016 Optimization of solar irradiated Fenton treatment of pesticide chlorpyrifos wastewater by response surface methodology. *Environmental Earth Sciences* **75**, 840.

Bahena, C. L. & Martínez, S. S. 2006 Photodegradation of chlorbromuron, atrazine, and alachlor in aqueous systems under solar irradiation. *International Journal of Photoenergy* **2006**, 6.

Ccanccapa, A., Masiá, A., Navarro-Ortega, A., Picó, Y. & Barceló, D. 2016 Pesticides in the Ebro River basin: occurrence and risk assessment. *Environmental Pollution* **211**, 414–424.

Chavoshani, A., Amin, M. M., Seidmohammadi, A. & Hashemi, M. 2018 *Peroxide Processes*.

Claver, A., Ormad, P., Rodríguez, L. & Ovelleiro, J. L. 2006 Study of the presence of pesticides in surface waters in the Ebro river basin (Spain). *Chemosphere* **64**, 1437–1443.

Dutta, A., Das, N., Sarkar, D. & Chakrabarti, S. 2019 Development and characterization of a continuous solar-collector-reactor for wastewater treatment by photo-Fenton process. *Solar Energy* **177**, 364–373.

EPA 2017 *Revised Human Health Risk Assessment on Chlorpyrifos*.

Estevez, E., Cabrera, M. d. C., Fernández-Vera, J. R., Molina-Díaz, A., Robles-Molina, J. & Palacios-Díaz, M. d. P. 2016 Monitoring priority substances, other organic contaminants and heavy metals in a volcanic aquifer from different sources and hydrological processes. *Science of The Total Environment* **551–552**, 186–196.

Fatima, R., Afridi, M. N., Kumar, V., Lee, J., Ali, I., Kim, K.-H. & Kim, J.-O. 2019 Photocatalytic degradation performance of various types of modified TiO_2 against nitrophenols in aqueous systems. *Journal of Cleaner Production* **231**, 899–912.

Faust, B. C. & Zepp, R. G. 1993 Photochemistry of aqueous iron (III)-polycarboxylate complexes: roles in the chemistry of atmospheric and surface waters. *Environmental Science & Technology* **27**, 2517–2522.

Hamm, R. E., Shull Jr, C. M. & Grant, D. M. 1954 Citrate complexes with iron (II) and iron (III). *Journal of the American Chemical Society* **76**, 2111–2114.

Hashemi, M., Amin, M. M., Sadeghi, S., Mengelizadeh, N., Mohammadi, F., Patastar, S., Chavoshani, A. & Rezaei, S. 2018 Coupling adsorption by NiO nanopowder with UV/H_2O_2 process for Cr (VI) removal. *Journal of Advances in Environmental Health Research* **5** (4), 210–219.

Heidari, M. R., Varma, R. S., Ahmadian, M., Pourkhosravani, M., Asadzadeh, S. N., Karimi, P. & Khatami, M. 2019 Photo-Fenton like catalyst system: activated carbon/$CoFe_2O_4$ nanocomposite for reactive dye removal from textile wastewater. *Applied Sciences* **9**, 963.

Herrero-Hernández, E., Andrades, M. S., Álvarez-Martín, A., Pose-Juan, E., Rodríguez-Cruz, M. S. & Sánchez-Martín, M. J. 2013 Occurrence of pesticides and some of their degradation products in waters in a Spanish wine region. *Journal of Hydrology* **486**, 234–245.

Hoseini, M., Nabizadeh, R., Nazmara, S. & Safari, G. H. 2016 Influence of under pressure dissolved oxygen on trichloroethylene degradation by the H_2O_2/TiO_2 process. *Journal of Environmental Health Science and Engineering* **11** (1), 38.

Hug, S. J., Canonica, L., Wegelin, M., Gechter, D. & Von Gunten, U. 2001 Solar oxidation and removal of arsenic at circumneutral pH in iron containing waters. *Environmental Science & Technology* **35**, 2114–2121.

ISO (International Organization for Standardization) 1988 ISO 6332:1988. Water quality – determination of iron. ISO, Geneva, Switzerland.

Jaafarzadeh, N., Ghanbari, F., Ahmadi, M. & Omidinasab, M. 2017 Efficient integrated processes for pulp and paper wastewater treatment and phytotoxicity reduction: permanganate, electro-Fenton and Co_3O_4/UV/peroxymonosulfate. *Chemical Engineering Journal* **308**, 142–150.

Koppenol, W. & Liebman, J. F. 1984 The oxidizing nature of the hydroxyl radical. A comparison with the ferryl ion (FeO^{2+}). *The Journal of Physical Chemistry* **88**, 99–101.

Leising, R. A., Brennan, B. A., Que Jr, L., Fox, B. G. & Munck, E. 1991 Models for non-heme iron oxygenases: a high-valent iron-oxo intermediate. *Journal of the American Chemical Society* **113**, 3988–3990.

Lenth, R. V. 2009 Response-surface methods in R, using rsm. *Journal of Statistical Software* **32**, 1–17.

Liu, T., Xu, S., Lu, S., Qin, P., Bi, B., Ding, H., Liu, Y., Guo, X. & Liu, X. 2019 A review on removal of organophosphorus pesticides in constructed wetland: performance, mechanism and influencing factors. *Science of The Total Environment* **651**, 2247–2268.

Malakootian, M. & Heidari, M. R. 2020 Green synthesis and application of heterogeneous iron oxide based nanoparticles for dairy wastewater treatment by Photo-Fenton processes. *Zeitschrift für Physikalische Chemie* **1**. https://doi.org/10.1515/zpc-2020-0002

Malakootian, M., Nasiri, A., Khatami, M., Mahdizadeh, H., Karimi, P., Ahmadian, M., Asadzadeh, N. & Heidari, M. R. 2019a Experimental data on the removal of phenol by electro-H_2O_2 in presence of UV with response surface methodology. *MethodsX* **6**, 1188–1193.

Malakootian, M., Nasiri, A. & Mahdizadeh, H. 2019b Metronidazole adsorption on $CoFe_2O_4$ /activated carbon@ chitosan as a new magnetic biocomposite: modelling, analysis, and optimization by response surface methodology. *Desalination and Water Treatment* **164**, 215–227.

Malakootian, M., Khatami, M., Mahdizadeh, H., Nasiri, A. & Amiri Gharaghani, M. 2020 A study on the photocatalytic degradation of p-nitroaniline on glass plates by thermo-immobilized ZnO nanoparticle. *Inorganic and Nano-Metal Chemistry* **50**, 124–135.

Manenti, D. R., Soares, P. A., Módenes, A. N., Espinoza-Quiñones, F. R., Boaventura, R. A. R., Bergamasco, R. & Vilar, V. J. P. 2015 Insights into solar photo-Fenton process using iron(III)–organic ligand complexes applied to real textile wastewater treatment. *Chemical Engineering Journal* **266**, 203–212.

Mendoza, J. A., Lee, D. H. & Kang, J.-H. 2017 Photocatalytic removal of gaseous nitrogen oxides using WO_3/TiO_2 particles under visible light irradiation: effect of surface modification. *Chemosphere* **182**, 539–546.

Mirzaei, A., Chen, Z., Haghighat, F. & Yerushalmi, L. 2017 Removal of pharmaceuticals from water by homo/heterogonous Fenton-type processes – a review. *Chemosphere* **174**, 665–688.

Naddafi, K., Nabizadeh, R., Martinez, S. S., Shahtaheri, S. J., Yaghmaeian, K., Badiei, A. & Amiri, H. 2018 Modeling of chlorpyrifos degradation by TiO_2 photo catalysis under visible light using response surface methodology. *Desalination and Water Treatment* **106**, 220–225.

Nogueira, R. F. P., Oliveira, M. C. & Paterlini, W. C. 2005 Simple and fast spectrophotometric determination of H_2O_2 in photo-Fenton reactions using metavanadate. *Talanta* **66**, 86–91.

Ou, X., Quan, X., Chen, S., Zhang, F. & Zhao, Y. 2008 Photocatalytic reaction by Fe(III)–citrate complex and its effect on the photodegradation of atrazine in aqueous solution. *Journal of Photochemistry and Photobiology A: Chemistry* **197**, 382–388.

Patel, H., Rawtani, D. & Agrawal, Y. K. 2019 A newly emerging trend of chitosan-based sensing platform for the organophosphate pesticide detection using acetylcholinesterase – a review. *Trends in Food Science & Technology* **85**, 78–91.

Ruales-Lonfat, C., Barona, J. F., Sienkiewicz, A., Vélez, J., Benítez, L. N. & Pulgarín, C. 2016 Bacterial inactivation with iron citrate complex: a new source of dissolved iron in solar photo-Fenton process at near-neutral and alkaline pH. *Applied Catalysis B: Environmental* **180**, 379–390.

Rush, J., Maskos, Z. & Koppenol, W. 1990 [12] Distinction between hydroxyl radical and ferryl species. *Methods in Enzymology* **186** 148–156.

Saini, R. & Kumar, P. 2016 Optimization of chlorpyrifos degradation by Fenton oxidation using CCD and ANFIS computing technique. *Journal of Environmental Chemical Engineering* **4**, 2952–2963.

Samet, Y., Hmani, E. & Abdelhédi, R. 2012 Fenton and solar photo-Fenton processes for the removal of chlorpyrifos insecticide in wastewater. *Water SA* **38**, 537–542.

Sun, Y. & Pignatello, J. J. 1993 Activation of hydrogen peroxide by iron (III) chelates for abiotic degradation of herbicides and insecticides in water. *Journal of Agricultural and Food Chemistry* **41**, 308–312.

Thimijan, R. W. & Heins, R. D. 1983 Photometric, radiometric, and quantum light units of measure: a review of procedures for interconversion. *HortScience* **18**, 818–822.

Watts, M. 2012 *Chlorpyrifos as a Possible Global POP*.

Zepp, R. G., Faust, B. C. & Hoigne, J. 1992 Hydroxyl radical formation in aqueous reactions (pH 3–8) of iron (II) with hydrogen peroxide: the photo-Fenton reaction. *Environmental Science & Technology* **26**, 313–319.

Zhang, M.-h., Dong, H., Zhao, L., Wang, D.-x. & Meng, D. 2019 A review on Fenton process for organic wastewater treatment based on optimization perspective. *Science of The Total Environment* **670**, 110–121.

First received 12 August 2020; accepted in revised form 11 November 2020. Available online 24 November 2020